Molecular Genetics and Metabolism Reports 42 (2025) 101176

Contents lists available at ScienceDirect

Molecular Genetics and Metabolism Reports

journal homepage: www.elsevier.com/locate/ymgmr

Identification of a new *COQ4* spliceogenic variant causing severe primary coenzyme Q deficiency

María Alcázar-Fabra [a,b,c], Elsebet Østergaard [d,e], Daniel J.M. Fernández-Ayala [a,b,c], María Andrea Desbats [f,g], Valeria Morbidoni [f,g], Laura Tomás-Gallado [h], Laura García-Corzo [a,b,c], María del Mar Blanquer-Roselló [a,b,c], Abigail K. Bartlett [i,j], Ana Sánchez-Cuesta [a,b], Lucía Sena [c], Ana Cortés-Rodríguez [k], María Victoria Cascajo-Almenara [a,b], David J. Pagliarini [j,l,m,n], Eva Trevisson [f,g], Sabine W. Gronborg [o], Gloria Brea-Calvo [a,b,c,*]

[a] *Andalusian Center of Developmental Biology (CABD), Universidad Pablo de Olavide-CSIC-JA, 41013 Seville, Spain*
[b] *Centre for Biomedical Research on Rare Diseases (CIBERER), Instituto de Salud Carlos III, 28029 Madrid, Spain*
[c] *Physiology, Anatomy and Cell Biology Department, Universidad Pablo de Olavide, 41013 Seville, Spain*
[d] *Department of Clinical Genetics, Copenhagen University Hospital Rigshospitalet, Blegdamsvej 9, 2100 Copenhagen, Denmark*
[e] *Department of Clinical Medicine, University of Copenhagen, Copenhagen, Denmark*
[f] *Clinical Genetics Unit, Department of Women's and Children's Health, University of Padova, 35128 Padova, Italy*
[g] *Istituto di Ricerca Pediatrica, Fondazione Città della Speranza, 35127 Padova, Italy*
[h] *Proteomics and Biochemistry Platform, Andalusian Centre for Developmental Biology (CABD), CSIC-Pablo de Olavide University, 41013 Seville, Spain*
[i] *Department of Biochemistry, University of Wisconsin–Madison, Madison, WI 53706, USA*
[j] *Department of Cell Biology and Physiology, Washington University School of Medicine, St. Louis, MO 63110, USA*
[k] *Bioenergetics and Cell Physiology Service (U729), Central Services of Research, University Pablo de Olavide, 41013 Seville, Spain*
[l] *Department of Biochemistry and Molecular Biophysics, Washington University School of Medicine, St. Louis, MO 63110, USA*
[m] *Department of Genetics, Washington University School of Medicine, St. Louis, MO 63110, USA*
[n] *Howard Hughes Medical Institute, Washington University School of Medicine, St. Louis, MO 63110, USA.*
[o] *Center for Inherited Metabolic Diseases, Department of Pediatrics and Adolescent Medicine and Department of Clinical Genetics, Copenhagen University Hospital Rigshospitalet, Blegdamsvej 9, 2100 Copenhagen, Denmark*

ARTICLE INFO

Keywords:
COQ4
Coenzyme Q10 deficiency
Spliceogenic variant
Mitochondrial disorder
Hybrid minigene
WES

ABSTRACT

Background and aims: Primary Coenzyme Q (CoQ) deficiency caused by *COQ4* defects is a clinically heterogeneous mitochondrial condition characterized by reduced levels of CoQ_{10} in tissues. Next-generation sequencing has lately boosted the genetic diagnosis of an increasing number of patients. Still, functional validation of new variants of uncertain significance is essential for an adequate diagnosis, proper clinical management, treatment, and genetic counseling.
Materials and methods: Both fibroblasts from a proband with *COQ4* deficiency and a *COQ4* knockout cell model have been characterized by a combination of biochemical and genetic analysis (HPLC lipid analysis, Oxygen consumption, minigene analysis, RNAseq, among others).
Results: Here, we report the case of a subject harboring a new variant of the *COQ4* gene in compound heterozygosis, which shows severe clinical manifestations. We present the molecular characterization of this new pathogenic variant affecting the splicing of *COQ4*.
Conclusion: Our results highlight the importance of expanding the genetic analysis beyond the coding sequence to reduce the misdiagnosis of primary CoQ deficiency patients.

Abbreviations: AntA, antimycin A; CNS, Central nervous system; CoQ, Coenzyme Q; FCCP, carbonyl cyanide-4-trifluoromethoxy-phenylhydrazone; HPLC, high-pressure liquid chromatography; MS, mass spectrometry; NGS, Next generation sequencing; OL, oligomycin; Rot, rotenone; VUS or VOUS, variants of unknown clinical significance; WES, whole exome sequencing; WGS, whole genome sequencing.

* Corresponding author at: Andalusian Center of Developmental Biology (CABD), Universidad Pablo de Olavide-CSIC-JA, Carretera de Utrera Km1, 41013 Seville, Spain.
E-mail address: gbrecal@upo.es (G. Brea-Calvo).

https://doi.org/10.1016/j.ymgmr.2024.101176
Received 5 August 2024; Received in revised form 6 December 2024; Accepted 9 December 2024
Available online 14 December 2024

1. Introduction

One of the most challenging aspects of the post-genome sequencing era is interpreting the pathogenicity of genomic variants for the molecular diagnosis of common and rare diseases. Therefore, efforts are continuously put in place to functionally validate DNA variants of unknown clinical significance (VUS or VOUS) found in disease-causing genes or new candidate genes identified through genome/ exome sequencing or analysis of specific gene panels. However, it is estimated that over half of the patients with a rare disease remain undiagnosed after exome or genome sequencing [1].

Pre-mRNA splicing is required to produce functional proteins in higher eukaryotes. Genetic changes can impact mRNA processing differently, causing skipped exons, the generation of alternative donor or acceptor splice sites, or retained introns, among others. Atypical pre-mRNA maturation can render aberrant and non-functional proteins. Thus, defective mRNA processing can result in disease. It is estimated that variants affecting pre-mRNA splicing account for at least 15 % of disease-causing variants. For certain genes, these variants can account for up to 50 % of the reported modifications [2]. However, Whole Exome Sequencing (WES) -which mostly gets information on the putative changes in the coding sequence and, at most, proximal intronic boundaries- or sequencing of a specific panel of genes are often the chosen molecular diagnostic tools for rare diseases. Consequently, disease-causing changes in non-coding sequences, such as unknown variants in promoters, enhancers, and deep intronic sequences, are potentially overlooked, preventing the molecular diagnosis of a probably non-negligible number of patients [3,4]. More comprehensive implementation of whole genome sequencing (WGS) has the potential to help overcome this limitation. However, functional interpretation and prioritization of non-coding variants, especially non-canonical splice sites, still represent a significant challenge [5,6].

Primary Coenzyme Q (CoQ) deficiencies constitute a group of rare conditions caused by autosomal recessive variants in any of the genes involved in the biosynthesis of this lipidic molecule (*COQ* genes) [7], which is central to mitochondrial metabolism [8], shuttling electrons from complexes I and II to complex III in the electron transport chain but also accepting electrons from other mitochondrial dehydrogenases. Outside mitochondria, CoQ is part of the antioxidant defense system in the plasma membrane, participating in the protection against ferroptosis [9]. In humans, Primary CoQ deficiencies are accompanied by a decrease in tissue levels of CoQ_{10} (the human isoform of CoQ, with 10 isoprene units) and are characterized by a vast spectrum of clinical manifestations, mainly affecting the central nervous system (CNS), peripheral nervous system, kidney, skeletal muscle, heart, and sensory organs [7,52]. Primary CoQ deficiency is a treatable disease since patients can be subjected to CoQ_{10} supplementation, but new treatments are under investigation, as the outcome of CoQ_{10} supplementation is variable, probably due to its high hydrophobicity and poor bioavailability [10–12].

The association of specific variants in the *COQ* genes with particular symptoms or disease prognosis could aid in the clinical management of patients. However, clear genotype-phenotype correlations have yet to be described, primarily due to the exiguity of identified patients and the difficulties in determining the impact of the particular genetic and epigenetic background on the disease manifestation [13]. To date, only around 600 patients have been identified worldwide harboring pathogenic variants in *PDSS1*, *PDSS2*, *COQ2*, *COQ4*, *COQ5*, *COQ6*, *COQ7*, *COQ8A*, *COQ8B* or *COQ9* [7,52], being most of the identified pathogenic variants located in the gene coding sequences; thus intronic variants affecting, *e.g.*, splicing may be overlooked.

One of the genes whose dysfunction causes primary CoQ deficiency is *COQ4*, which has recently been demonstrated to be required for the C1 oxidative decarboxylation of the CoQ precursor [14]. COQ4 patients predominantly exhibit neonatal-onset severe neurological impairment, often accompanied by cardiomyopathy and respiratory distress, with no evidence of renal involvement [7,15,52].

Here, we report and characterize a case of a spliceogenic variant in the *COQ4* gene, expanding the catalog of pathogenic variants for this gene. In the long term, this will contribute to a more rapid diagnosis of patients and their earlier treatment.

2. Material and methods

2.1. Whole exome analysis

WES was conducted using DNA isolated from blood with the Ion AmpliSeq™ exome RDY kit (Thermo Fisher, Waltham, MA, USA). Library preparation was carried out with the IonChef, followed by sequencing using the IonProton system (Thermo Fisher). Base calling, read pre-processing, short read alignment, and variant calling were completed using the Torrent Suite, including the Torrent Variant Caller (Version 4.4–5.0) (Thermo Fisher). Genomic variants were annotated and filtered using VarSeq (GoldenHelix, Bozeman, MT, USA). NM_016035.5 was used as the reference sequence for the *COQ4* transcript, and NP_057119.3 for the COQ4 protein for variant nomenclature.

2.2. Cell culture

Fibroblasts derived from a skin biopsy from the proband (PF) and age-matched control fibroblasts (HDF neonatal, ATCC) were cultured in Gibco™ DMEM (Dulbecco's Modified Eagle Medium) with 1 g/L glucose, supplemented with 10 % (*v*/v) fetal bovine serum (FBS) and 1 % (v/v) Gibco™ Antibiotic-Antimycotic cocktail (Ab). All the experiments were conducted using cells with passage numbers below 15. Informed consent for biological sample collection and genetic studies was obtained in accordance with the Declaration of Helsinki. All procedures were approved by the Andalusian Biomedical Research Ethics Coordinating Committee (Ref # 0418-N-20, 29/04/2020).

Human HEK293T-Rex/Flp-In™ parental cells (ThermoFisher Scientific) and derived *COQ4* KO cells were cultured in high glucose DMEM supplemented with 10 % tetracycline free FBS (Tet-FBS), 1 % Ab, 10 μM uridine, and maintained in 15 μg/mL of Blasticidin (Blasticidin S HCl, 10 mg/mL, Thermo Fischer Scientific) and 100 μg/mg Zeocin (Zeocin™ Selection Reagent, 100 mg/mL, Thermo Fischer Scientific). Transfected HEK293T cells were maintained with 15 μg/mL of Blasticidin and 100 μg/mg Hygromycin B (Sigma).

2.3. Oxygen consumption rate (OCR) measurements

OCR was measured using a Seahorse XF24 Extracellular Flux Analyzer (Agilent). Briefly, 50×10^3 cells were seeded onto Seahorse 24-well plates 24 h before the assay. On the day of the experiment, the plate was equilibrated with Seahorse XF base medium supplemented with 1 g/L glucose, 2 mM glutamine, and 1 mM sodium pyruvate for 1 h at 37 °C without CO_2. OCR was determined under basal conditions and after the sequential injection of the inhibitors (loaded in the pre-hydrated cartridge): 4 μM oligomycin (OL, inhibitor of ATP synthase), 1 μM carbonyl cyanide-4-trifluoromethoxy-phenylhydrazone (FCCP, uncoupling agent), 1 μM rotenone (Rot, CI inhibitor) and 2.5 μM antimycin A (AntA, CIII inhibitor). Cells were harvested and counted after the assay to normalize respiration rates.

2.4. Generation of HEK293T COQ4 KO cells

A Paired nickases CRISPR/Cas9 3-plasmid strategy was employed to generate the *COQ4* KO in a HEK293T-Rex/Flp-In wild type background. The cells were transfected with a pCMV-Cas9D10A-GFP plasmid (Sigma), which expresses the nickase-GFP, and two pU6-gRNA plasmids (Sigma), each containing a different target sequence in *COQ4* exon 2 (Table S1). The gRNAs for the target sequences were designed using the CRISPR-design tool from Zhang Lab (http://crispr.mit.edu). Potential

off-target sites of the different pairs of gRNAs were analyzed with the same tool, predicting 0 off-target sites for each of the 4 pairs of Forward and Reverse gRNAs used (gRNA1-gRNA3, g-RNA1-gRNA4, gRNA2-gRNA3, gRNA2-gRNA4).

The CRISPR plasmids transfection protocol was adapted from Ran et al. [16] and conducted using Lipofectamine 3000 (LFA) (ThermoFisher Scientific) in 24-well plates following the manufacturer's instructions. Transfections with the 4 combinations of plasmids containing the gRNAs were performed along with the pCMV-Cas9D10A-GFP plasmid in equimolar ratios, with a maximum total DNA amount of 500 ng. Forty-eight hours after transfection, GFP-positive single cells were FACS-sorted (BD Facsaria cell sorter), collected in complete high glucose DMEM medium supplemented with 10 μM uridine, and diluted to plate 1 single cell per well in a 96-well plate. After expanding cell populations, genomic DNA was isolated from 80 % of cells in a confluent 12-well plate using the DNeasy Blood & Tissue Kit (Qiagen).

The KOD Hot Start Master Mix (Novagen) was used to specifically amplify the targeted *COQ4* or *EMX1* (as a positive control) genomic sequences (Table S2) by PCR. After the separation in a 1,8 % agarose gel, amplicons were gel-purified, A-tailed with a Taq polymerase (Horse-Power Taq polymerase, Canvax), ligated into pGEM-T Easy Vector (Promega), and transformed into DH5α bacteria. A minimum of 5 bacterial clones were sequenced per each tested cell line. HEK293T *COQ4* KO cell line was confirmed not to express COQ4 protein by Western Blot (anti COQ4 antibody (Sigma HPA042945), 1/1000).

2.5. Generation of HA-tagged versions of COQ4 and site-directed mutagenesis

COQ4 was amplified from a plasmid containing the human *COQ4* coding sequence using specific primers to introduce the HA tag and the restriction enzyme sites for *Hin*dIII and *Xho*I (Table S2). The *COQ4*-HA was then cloned into pcDNA5 (ThermoFisher Scientific). Site-directed mutagenesis was conducted using the QuikChange II XL Site-Directed Mutagenesis kit (Agilent) with specific PCR primers (Table S2).

2.6. Generation of stable inducible cell lines expressing COQ4 variants

HEK293T *COQ4* KO cells were transfected with different *COQ4* versions. 70–80 % confluent cells in 6-well plates were transfected with Lipofectamine 3000 reagent (LFA, ThermoFisher Scientific), following the manufacturer's instructions. Briefly, each well was transfected with 600ul of LFA-DNA complexes (a mixture of pOG44 and pCDNA5 with each of the *COQ4* versions (ratio 9:1, 1500 ng), LFA and P3000 reagent) on Gibco Opti-MEM™ (Thermo Fischer Scientific). 24 h after transfection, the medium was replaced by high glucose DMEM supplemented with 10 % Tet-FBS, 1 % Ab, 15 μg/mL Blasticidin. 48 h after transfection, transfected clones were subjected to selection by changing the medium to high glucose DMEM with 10 % Tet-FBS, 1 % Ab, 10 μM uridine, 15 μg/mL of Blasticidin, and 100 μg/mg of Hygromycin B (Sigma). The transgene expression was induced with 0.1–0.5 ng/mL of doxycycline for 24 h and checked by Western Blot (anti COQ4 antibody (Sigma HPA042945) 1/1000).

2.7. Western blotting and immunodetection

Western blotting analysis was performed after denaturing acrylamide electrophoresis. Proteins in the gel were transferred onto a methanol-activated polyvinylidene difluoride (PVDF) membrane (Immobilon. Millipore) by semi-dry transfer (Trans-Blot® SD Semi-Dry Transfer Cell, Bio-Rad) at 25 V for 1 h in transfer buffer TG (25 mM Tris-HCl, 192 mM Glycine, 20 % methanol (*v*/v) and 0.025 % SDS) (Bio-Rad).

The membranes were blocked with 5 % milk in TTBS (TBS (Tris-buffered saline) with 0.05 % Tween-20) for 1 h at room temperature (RT) and subsequently washed in TTBS. Membranes were incubated at 4 °C overnight with different specific antibodies diluted at the appropriate concentrations in 5 % milk in TTBS. After further washes in TTBS, membranes were subsequently incubated with species-appropriate secondary antibody conjugated with horseradish peroxidase (HRP) diluted to 1:5000 in 5 % milk in TTBS. Finally, membranes were developed with Immobilon Crescendo Western HRP substrate (Millipore) and visualized with ChemiDocTM XRS+ Imaging System (Bio-Rad).

2.8. Steady-state CoQ level measurements

Lipid extraction was performed from 0.5 mg of total cell homogenate protein following standard procedures [17] using CoQ_6 as an internal standard. CoQ_{10} content was analyzed by injecting lipid extracts in an HPLC system, as described elsewhere [17], with a guard cell installed after the injection valve to oxidize the sample completely before chromatographic analysis. Lipids separation was conducted using a gradient method in a C18 Reverse Phase column HPLC system (5 μm, 150 × 4.6 mm) with 20 mM AcNH4 pH 4.4 in methanol (solvent A) and 20 mM AcNH4 pH 4.4 in propanol (solvent B) as the mobile phase. An 85:15 solvent mixture (A:B ratio) and a 1.2 mL/min flow rate were used as starting conditions. Then, the mobile phase gradually turned into a 50:50 ratio as the flow rate decreased to 1.1 mL/min (ramp from minute 6 to minute 8). After 20 min (total run time) at 40 °C, the columns were re-equilibrated to the initial conditions for three additional minutes. CoQ_{10} levels were detected by an electrochemical detector (ECD) (channel 1 set to −700 mV and channel 2 set to +500 mV) or radio-flow detector (LB 509 with a solid cell YG 150 Al-U4D (Berthold Technologies)).

2.9. CoQ_{10} biosynthesis rate measurements

The CoQ_{10} biosynthesis rate was determined by measuring the incorporation of radioactive ^{14}C into CoQ_{10}. Cell cultures were incubated with 7.2 nM of the radiolabelled [^{14}C]-pHB, the precursor of the benzoquinone ring, for 72 h. Labeled-CoQ_{10} content was analyzed by lipid extract injection in HPLC as described above. [^{14}C]-pHB was in-house chemically synthesized from ^{14}C-tyrosine [18].

2.10. Targeted mass spectrometry CoQ intermediary analysis

Flash-frozen cell pellets were thawed and resuspended in 100 μL of PBS. A 5 μL aliquot of this resuspension was reserved for BCA assay to normalize the protein content. 600 μL of methanol with 0.1 μM CoQ_8 internal standard (Avanti Polar Lipids) was added to each sample. Cells were lysed by shaking for 5 min at 4 °C using a Disruptor Genie set to 3000 rpm. For lipid extraction, 400 μL of petroleum ether was mixed with the sample and shaken for 3 min. The samples were centrifuged for 2 min at 1000*g* and 4 °C, and the upper ether layer was transferred to a new tube. This extraction process was repeated twice, and the combined ether layers were evaporated under argon gas for 30 min at RT. Extracted dried lipids were resuspended in the mobile phase (78 % methanol, 20 % isopropanol, 2 % 1 M ammonium acetate pH 4.4 in water) and placed in amber glass vials with inserts. LC-MS analysis was performed using a Thermo Vanquish Horizon UHPLC system coupled to a Thermo Exploris 240 Orbitrap mass spectrometer. The LC separation utilized a Vanquish binary pump system (Thermo Fisher Scientific) with a Waters Acquity CSH C18 column (100 mm × 2.1 mm, 1.7 μm particle size) maintained at 35 °C under a 300 μL/min flow rate. Mobile phase A was composed of 5 mM ammonium acetate in acetonitrile:H_2O (70:30, *v*/v) with 125 μL/L acetic acid, while mobile phase B consisted of 5 mM ammonium acetate in isopropanol:acetonitrile (90:10, v/v) with the same additive. For each sample run, the gradient started with 2 %mobile phase B for 2 min, then increased to 30 % over 3 min, further rising to 50 % over 1 min, 85 % over 14 min, and finally to 99 % over 1 min, holding at 99 % for 4 min. The column was then re-equilibrated for 5 min at 2 % mobile phase B before the next injection. Five μL of each sample were

injected by a Vanquish Split Sampler HT autosampler (Thermo Fisher Scientific) at 4 °C. Ionization was achieved using a heated ESI source with a vaporizer temperature of 350 °C. Sheath gas was set to 50 units, auxiliary gas to 8 units, sweep gas to 1 unit, and the spray voltage was set to 3500 V for positive mode and 2500 V for negative mode. The inlet ion transfer tube temperature was maintained at 325 °C with a 70 % RF lens. For targeted analysis, the MS was operated in positive parallel reaction monitoring mode with polarity switching acquiring scheduled, targeted scans to CoQ_{10} (*m/z* 863.6912), CoQ_8 (m/z 727.566), CoQ_6 (m/z 591.4408), and CoQ intermediates: demethoxy-coenzyme Q (DMQ_{10}; m/z 833.6806), demethyl-coenzyme Q ($DMeQ_{10}$; m/z 849.6755), demethoxy-demethyl-coenzyme Q ($DDMQ_{10}$; m/z 836.6915), 3-decaprenyl-4-hydroxybenzoate ($_{10}$P-HB; m/z 817.6504) and 3-decaprenyl-1,4-benzoquinone (PBQ_{10}; m/z 789.6555). MS acquisition parameters include resolution of 15,000, stepped HCD collision energy (25 %, 30 %, 40 % for positive mode and 20 %, 40 %, 60 % for negative mode), and 3 s dynamic exclusion. Automatic gain control targets were set to standard mode. The resulting CoQ intermediate data were processed using TraceFinder 5.1 (Thermo Fisher Scientific).

2.11. Spliceogenicity in silico prediction

Splicing Prediction in Consensus Elements (SPiCE) [19], SpliceAI [20], HSP [21], Spliceator [22], and the NetGene2 [23] prediction tools were used to *in silico* predict the spliceogenicity of the intronic variant.

2.12. Hybrid minigene assay

COQ4 complete exon 5 and 100 bp of the upstream and downstream introns 4 and 5 were amplified from the proband and control genomic DNA. Fragments were cloned into the β-globin intron 2 contained in the β-globin vector to build the minigene vectors [24]. HEK293T cells that do not express β-globin were transfected with the wild type or the mutated minigene using Lipofectamine 2000 (ThermoFisher Scientific) according to the manufacturer's instructions. Transfection of the empty vector was used as a negative control. After 24 h, total RNA was extracted with TRIzol (ThermoFisher Scientific) and retrotranscribed using SuperScript II reverse transcriptase (ThermoFisher Scientific). The resulting cDNA was amplified using specific primers for the β-globin gene, designed on exon 2 (forward) and exon 3 (reverse). PCR products were separated on a 2 % agarose gel, and densitometric analysis was performed using ImageJ software. Bands were excised from the gel and sequenced by Sanger.

2.13. RNA sequencing

Total RNA was extracted from the proband and control fibroblast pellets using TRIzol (ThermoFisher Scientific). At least 2 μg of RNA per sample were submitted to Novogene Europe (Cambridge, United Kingdom) in triplicates. Novogene prepared the libraries and performed the paired-end sequencing of the samples with Illumina NovaSeq 6000 (150 nt read length). The obtained sequences were mapped to the human reference genome GRCh38 assembly. The Integrative Genomics Viewer (IGV) software (Broad Institute and UC San Diego) was used for data visualisation [25], focusing on *COQ4, COQ2,* and *TFAM* transcripts, and reads for each exon and exon-exon junction were counted.

2.14. Reverse transcription and transcript variants amplification

1 μg of DNase-treated RNA was retrotranscribed with the iScript Select cDNA Synthesis Kit (Bio-Rad) by using oligo$(dT)_{20}$ primer mix to obtain the complementary DNA (cDNA). A first-strand cDNA amount equivalent to 150 ng of starting RNA was used for subsequent PCR reactions. Specific primers for WT or 10 nt-deletion in exon 1 were used to distinguish amplicons coming from each allele by standard PCR (Table S2). After agarose gel running of the RT-PCR products, bands were excised, cloned in pGEM-T Easy Vector (Promega) and sequenced.

2.15. Statistical analysis

All results were expressed as mean ± SD, unless otherwise specified. Data analysis was performed with GraphPad Prism 8.0. Samples were assumed to come from a normal distribution. In the case of comparison between two groups, we used unpaired two-tailed *t*-test with a Welch's correction. Multiple samples were compared using a one-way (1 group) or two-way ANOVA (2 or more groups), with Sidak's or Dunnett's multiple comparison post-hoc tests (depending on the nature of the data and the comparisons). *P*-values <0.05 were considered statistically significant.

3. Results

3.1. Case clinical presentation

The proband was the first child of healthy and unrelated parents. Pregnancy was uneventful, and birth was induced and uncomplicated at 41 + 6 weeks of gestation with Apgar values of 9 and 10 after one and five minutes, respectively. Birth weight was 3076 g (z = −0,35), length 48 cm (z = −0,82), and head circumference 33 cm (z = −1,07). Directly after birth, the female neonate was noted to have hypertonia in extremities. 6 h after birth, periodic breathing with upper airway obstruction was noted, and the proband was transferred to the neonatal care unit. The respiratory situation stabilised, but the patient was found to have flexion contractures of both elbows and knees, contractures over ankle joints with dorsal flexion, as well as tightly closed hands with adducted thumbs. Muscle tone was increased. A cerebral MRI was performed when the proband was 3 days old and revealed severe volume reduction of the cerebral and cerebellar white matter but otherwise normal anatomy. Myelinisation was delayed, with signs of myelinization in the dorsal brainstem only. The initial ophthalmological examination did not show signs of ocular pathology. The patient underwent a series of diagnostic tests, including routine clinical biochemistry, broad metabolic screening, array CGH (comparative genomic hybridization) analysis, and investigations for congenital infections, all with normal results. Trio whole exome sequencing (WES) was ordered. At the age of 4 weeks, the patient developed epileptic seizures, initially treated efficiently with levetiracetam, but requiring the addition of clobazam shortly after. Because of severe feeding difficulties, a nasogastric tube was placed at age 5 weeks and converted to a percutaneous gastric tube at age 8 months. Because of increased muscle tone, irritability, periods of unconsolable crying, and apnoeic spells, oral baclofen and later gabapentin treatment were added to her treatment regimen with limited success. She later developed epileptic spasms, and vigabatrin treatment was started. She also manifested severe neuromuscular scoliosis. WES revealed a putative diagnosis of *COQ4* deficiency (see next paragraph), and the patient was started on CoQ_{10} treatment (ubiquinol, 30 mg/kg/d in 3 doses) from the age of two months old. Echocardiography was normal. From the age of 8 months, patients' irritability and muscular hypertonia were increasing and difficult to manage despite polypharmacy. Treatment with L-Dopa did not ameliorate the situation and was withdrawn because of increasing irritability. Chloralhydrate, diazepam, morphine, and clonazepam were needed to treat severe irritability and high muscle tone but were only partly efficient. Also, at 8 months of age, respiratory problems were observed, with increasing difficulties with airway secretions and reduced coughing. The patient was referred to close follow-up with the pediatric palliative care team from 12 months of age. Overall, the proband only showed very limited progress in psychomotor development within the first months, especially regarding eye contact, and then regression from about 8 months of age, with loss of limited eye contact and reactions to parents and other caretakers. Head circumference showed very slow growth, and was at z − 4,64 at 12 months (with normal weight (z − 0,68) and length at z −

2,31). At 15 months of age, repeating episodes of severe upper airway obstruction not amenable to conservative treatment occurred, and at 16 months, the patient deceased, possibly due to airway obstruction.

3.2. Pathogenicity of *COQ4* identified variants

In trio WES on the proband and her parents' genomic DNA revealed that she was compound heterozygous for two variants in the *COQ4* gene. One of the variants is a deletion of 11 nucleotides in exon 1 (c.23_33delTCCTCCGTCGG), predicted to generate a frameshift and an early truncated protein (p.Val8Alafs*19). The second *COQ4* variant is an intronic single nucleotide variant (SNV) in intron 5, c.532 + 6 T > A.

The c.23_33delTCCTCCGTCGG variant has been previously described in compound heterozygosity with an allele harboring two missense variants, c.311G > T and c.356C > T (p.Asp111Tyr and p.Pro119Leu), both predicted to be pathogenic by different *in silico* tools. This combination was observed in a subject who presented with a birth-onset encephalopathy associated with seizures, hypotonia, developmental delay, hearing loss, delayed visual maturation, hypertrophic cardiomyopathy, and bradycardia. The patient succumbed after a respiratory failure at 4 months of age [26].

The c.23_33delTCCTCCGTCGG allele is expected to result in a loss-of-function protein as the deletion occurs very early in the sequence (p.Val8Alafs*19). A stable *COQ4* knockout (KO) HEK293T inducible cell line expressing the cDNA of this variant was generated using the Flp-In system to check its pathogenicity. As expected, after induction, the protein was undetectable by Western Blot (Fig. 1A), and cells were unable to restore wild-type CoQ_{10} levels (Fig. 1B) in the *COQ4* KO background. Of note, the small amounts of CoQ_{10} observed are probably derived from the culture medium and not endogenously synthesized since there is no detectable incorporation of radioactivity when cells are fed with radioactive [^{14}C]-pHB, the head precursor of CoQ (Fig. S1). These results confirm the c.23_33delTCCTCCGTCGG cDNA does not produce protein and, thus, induces a defect in CoQ_{10} biosynthesis.

In contrast, cells expressing the *COQ4* cDNA harboring the missense variant causing the p.Leu52Ser change found in a published cohort of *COQ4* patients [27] and used as a control in our functional studies had detectable protein amounts after induction (Fig. 1A). Doxycycline-induced overexpression of the p.Leu52Ser protein rescued CoQ_{10} levels in a dose-dependent manner, suggesting that, unlike the p.Val8Alafs*19 variant, the p.Leu52Ser one is a functional but less efficient protein (Fig. 1B). Of note, cells transfected with the WT allele but not induced with doxycycline expressed comparable amounts of protein as the HEK293T WT cells and recovered wild-type CoQ_{10} levels, indicating that the leaky expression of the gene is enough to restore CoQ_{10} synthesis. Induction of the transgene resulted in a high overexpression, which explains the recovery of wild-type levels of CoQ_{10} by the hypomorphic p.Leu52Ser variant in this condition. Interestingly, we observed that cells lacking COQ4 accumulate an ECD-detectable compound which does not show the same retention time as demethoxy-coenzyme Q (DMQ_{10}), the substrate of the hydrolase COQ7 that is typically accumulated in *COQ7* patients and has previously been detected in probands

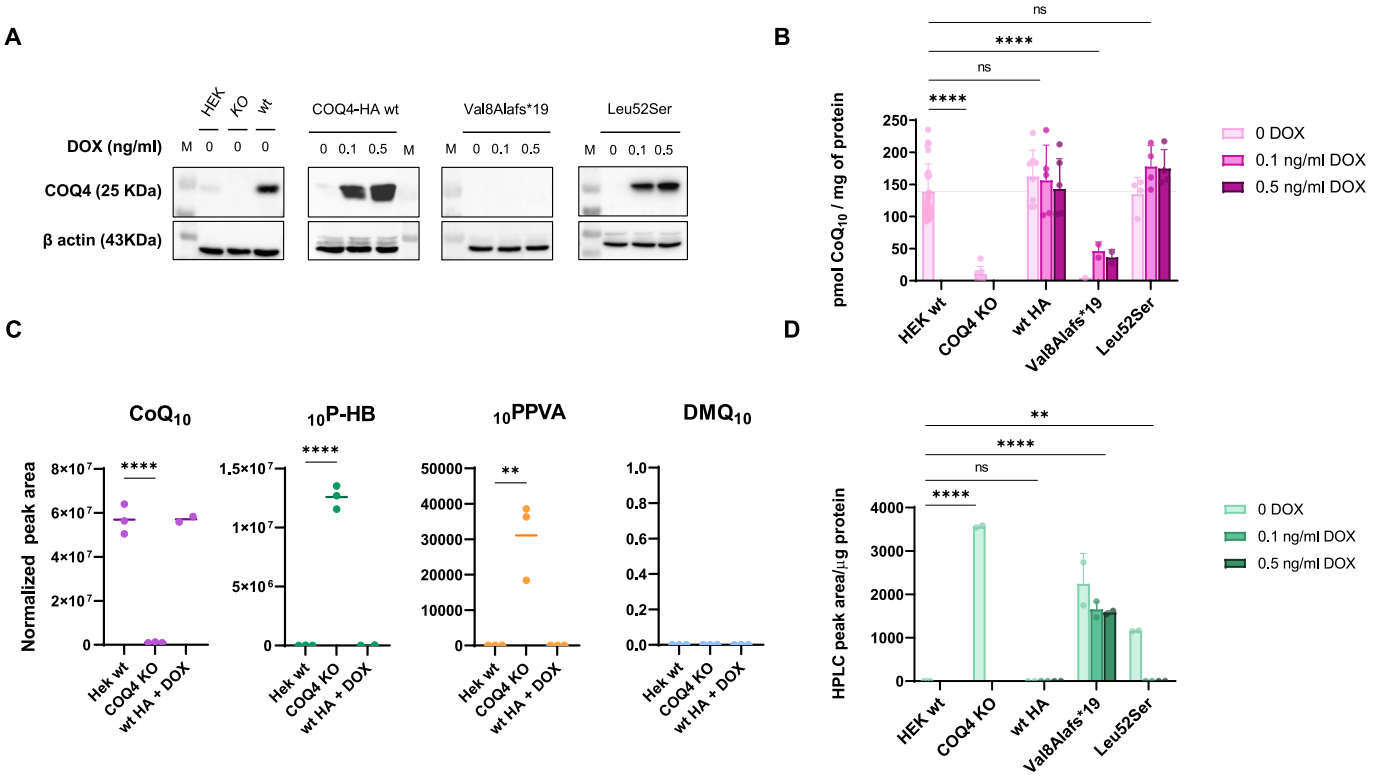

Fig. 1. *COQ4* KO cells transfected with *COQ4* wild type and variants found in patients recover COQ4 protein expression and CoQ_{10} levels in different degrees and accumulate a CoQ_{10} biosynthesis intermediary. **A.** Levels of COQ4 proteins in HEK293T WT (HEK), *COQ4* KO (KO), and *COQ4* KO transfected with WT *COQ4* (WT) or with the HA-tagged WT (*COQ4*-HA wt) or the c.23_33delTCCTCCGTCGG (p.Val8Alafs*19) *COQ4* variant. The p.Leu52Ser variant is used as a control of the system. Membranes were developed with an antibody against the COQ4 protein. Protein expression was induced with doxycycline (DOX) for 24 h. **B.** CoQ_{10} levels in HEK WT, *COQ4* KO, *COQ4* KO cells transfected with HA-tagged WT *COQ4* and patients' mutant versions of COQ4 p.Val8Alafs*19 and p.Leu52Ser (Mean and SD are represented; Two-way ANOVA, Dunnett's multiple comparison test (each transfected cell line (induced+non-induced) *vs.* HEK WT); *p* values: ****, $p < 0.0001$). **C.** CoQ_{10}, $_{10}$P-HB, $_{10}$PPVA and DMQ_{10} levels measured by targeted mass spectrometry of WT HEK293T (HEK wt), *COQ4* KO and *COQ4* KO cells transfected with HA-tagged WT *COQ4* induced with 0,5 ng/mL doxycycline (wt HA + DOX) (Scatter dot plots with means are represented; One-way ANOVA, Dunnett's multiple comparison test; p values: **, $p < 0.002$; ****, $p < 0.0001$). **D.** Pre-CoQ_{10} levels in HEK293T WT, *COQ4* KO, *COQ4* KO cells transfected with HA-tagged WT COQ4 (wt HA) and patients' mutant versions of COQ4 (p.Val8Alafs*19 and p.Leu52Ser) (Mean and SD are represented; Two-way ANOVA, Dunnett's multiple comparison test (each transfected cell line (induced+non-induced) *vs.* HEK WT); p values: ****, $p < 0.0001$).

with pathogenic variations in *COQ4* [28] (Figs. S2 and S3). Mass spectrometry (MS) analysis of lipid extracts confirmed that DMQ_{10} is not present in *COQ4* KO cells and that they mainly accumulate 3-decaprenyl-4-hydroxybenzoate ($_{10}$P-HB), the product of *COQ2*, which has been recently shown to accumulate in *COQ4*-defective cells and some *COQ4* patients [14]. Traces of polyprenyl-vanillic acid ($_{10}$PPVA), the substrate of COQ4, are also detected in *COQ4*-defective cells but not in HEK293T WT and those rescued by expression of wild-type COQ4 (Fig. 1C and S3). The main accumulated intermediary disappeared when the WT *COQ4* HA-tagged version was expressed in the *COQ4* KO cells (Fig. 1C and D) but was detected when both p.Val8Alafs*19 and p.Leu52Ser variants were expressed in this background, meaning that the enzymatic activity of these forms is probably slowed down (Fig. 1D).

The second *COQ4* variant identified in the proband under study is an intronic SNV, c.532 + 6 T > A (ClinVar RCV002226918.2), that has not been previously described in the literature and is classified as very rare in the GnomAD v4.0 dataset (MAF, maximum allele frequency of 0.00001470 in the European non-Finnish population). Interestingly, it is located close to the predicted 5′ donor splice site of intron 5 of *COQ4*. Thus, c.532 + 6 T > A molecular pathogenetic mechanism may rely on the alteration of *COQ4* pre-mRNA splicing. *In silico* spliceogenicity prediction tool, SPiCE [19] predicts the intronic variant c.532 + 6 T > A to have a moderate probability of altering splicing (0.734) but close to the threshold ThSp (0.749), which marks the highest likelihood of spliceogenicity (Fig. S4). In contrast, NetGene2 only predicts a slight weakness of the donor site, while SpliceAI [23] indicates no spliceogenicity to the c.532 + 6 T > A variant (score 0,10) [20].

3.3. Functional and biochemical characterization of proband's cells

Biochemical characterization of proband samples was performed to functionally validate the pathogenicity of the identified *COQ4* variants. The steady-state CoQ_{10} levels were found to be severely reduced both in skeletal muscle (154.37 pmol CoQ_{10}/mg of protein, control range 300–700) and skin fibroblasts (more than 50 %deficiency) (Fig. 2A). Citrate synthase activity was also found to be slightly reduced in skeletal muscle (82.8 CS units/L, control range 88–240), indicating that this primary CoQ_{10} defect could lead secondarily to suboptimal mitochondrial performance in muscle.

Measuring the incorporation rate of labeled precursors in the form of CoQ_{10} allows the unveiling of defects in the biosynthesis process itself. Incorporation of radiolabelled [^{14}C]-pHB, the quinone head precursor of CoQ, revealed a severe defect in CoQ_{10} biosynthetic rate (Fig. 2B), and the accumulation of a radioactive peak with an earlier retention time than CoQ_{10} and coincident with the extra peak detected in the *COQ4* KO HEK293T cells by the ECD (Fig. S1). MS analysis of proband's fibroblasts detected low amounts of $_{10}$P-HB, but no other biosynthetic intermediary analyzed (Fig. 2C-D).

COQ4 protein levels were drastically reduced in the proband fibroblasts (PF) compared to matched-age control fibroblasts (Fig. 2E). Oxygen consumption rate (OCR) was measured in PF to determine the cells' respiratory capacity. Basal respiration, proton leak, and coupled respiration levels were unaffected. In contrast, maximal respiration rate and spare capacity were significantly decreased in PF, indicating that patients' cells are unable to respond appropriately when the respiration machinery is pushed to be over-activated (Fig. 2F-G).

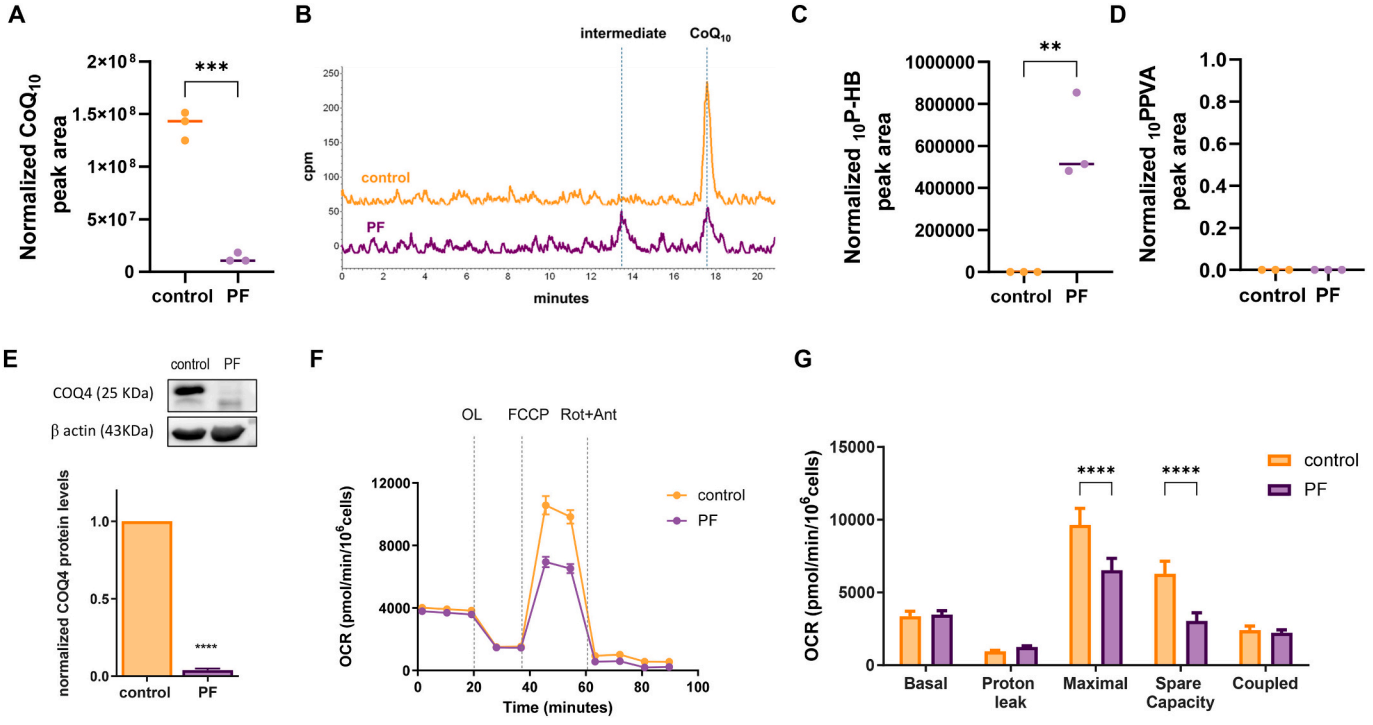

Fig. 2. Quinone content, COQ4 protein levels, and respiratory capacity of COQ4 proband's fibroblasts. **A.** Mass spectrometry analysis of CoQ_{10} steady-state levels in controls and proband's fibroblasts (PF) (Scatter dot plot with means is represented; Unpaired two-tailed *t*-test; ***, p value<0.0005). **B.** HPLC-radioactivity chromatogram showing the incorporation of ^{14}[C]-pHB to the quinone extract. While control cells show a radioactive CoQ_{10} peak, PF present 2 peaks, one corresponding to CoQ_{10}, and another of lower retention time (13–13.5 min), corresponding to an intermediate molecule of CoQ_{10} synthesis. **C.** Mass spectrometry analysis of control and COQ4 PF shows that the latter accumulate $_{10}$P-HB (Scatter dot plot with means is represented; Unpaired two-tailed t-test; **, p value<0.05). **D.** Mass spectrometry analysis shows that $_{10}$PPVA is undetectable in both control and patient's cells. A scatter dot plot with means is represented. **E.** COQ4 protein levels in whole fibroblast lysates and western blot quantification by densitometry (Unpaired two-tailed t-test; p value<0.0001). An antibody against beta-actin (43KDa) was used as a loading control. **F.** Representative OCR traces of proband (PF) and control cells measured by Seahorse. Lines indicate the addition of the individual inhibitors. OL (oligomycin 4 μM); FCCP (Carbonyl cyanide 4-(trifluoromethoxy)phenylhydrazone 1 μM); Rot (rotenone 1 μM); Ant (antimycin A 2.5 μM). **G.** Normalized respiratory parameters of control and PF. ± SD. PF *vs.* control cells (Mean ± SD are represented; Two-way ANOVA with Sidak's multiple comparison test. ****, p value<0.0001).

3.4. Minigene analysis of c.532 + 6 T < a variant spliceogenicity

Minigene constructs [29] were used to analyze the effect of the c.532 + 6 T > A variant on *COQ4* splicing *in vitro*. Two versions of *COQ4* exon 5 flanked by 100 bp upstream and downstream sequence, containing the region of interest, were cloned into the β-globin minigene and expressed in HEK293T cells (Fig. 3A). The expression of the wild type and the c.532 + 6 T > A variant minigene constructs yielded two products but in significantly different proportions. The mutated construct predominantly produced a fragment lacking exon 5 (91 % of the total amplification), but also the wild-type fragment in a lower proportion (9 % of the total amplification) (Fig. 3B). Interestingly, a fragment lacking exon 5 was also generated from the wild-type construct, although in a significantly smaller proportion. Thus, non-canonical splicing may naturally occur at low levels, although c.532 + 6 T > A variant probably increases the frequency of abnormal mRNA processing. These results confirm that the variant under study is hypomorphic and alters transcript maturation, predominantly leading to exon 5 skipping, at least when considered in this specific *in vitro* context.

3.5. RNAseq analysis of COQ4 mRNA isoforms

The minigene assay only studies the effect of the variant in the context of a single and isolated exon, limiting the information on the impact of the variant in the whole transcript. To overcome this limitation, a deeper transcriptomic analysis in control and PF was performed. Surprisingly, a broader splicing defect was detected in the *COQ4* transcript. All splicing events were quantified as a percent spliced (the percentage of a gene's mRNA transcripts that include a specific splice junction) (Fig. S5). The PF showed fewer reads of mainly exon 3, but also exon 5 (Fig. 3C-D), indicating that these exons are more frequently excised in PF. Interestingly, an unexpected splicing event was also observed in the middle of intron 2, leading to an abridged transcript in both control and PF.

We checked splicing events in *COQ2* and *TFAM* mRNAs, to exclude a general splicing defect, but no differences between the control and proband samples were found (Fig. S5). To discard an effect of mRNA nonsense-mediated decay (NMD) and check whether both alleles were being produced in the same amount, the number of reads of the region that carry the 11-nucleotide deletion, c.23_33delTCCTCCGTCGG, was counted and compared with the number of reads of the 11 nucleotides downstream this deletion (control region, c.33–42) (Table S3). In the control fibroblasts, both regions had the same number of reads, while in the patient's RNA, the control region had twice the number of reads compared to the deletion. This observation suggested that *COQ4* mRNA is generated from both alleles in a 1:1 proportion. However, this result does not exclude the possibility that the splicing variants are also produced from the c.23_33delTCCTCCGTCGG allele.

3.6. Analysis of the transcript isoforms derived from the different COQ4 alleles in the proband cells

The minigene approach predicted that variant c.532 + 6 T > A would result in exon 5 skipping. However, the RNAseq analysis shows a more general *COQ4* splicing defect. The transcriptomic analysis is unable to distinguish which allele the different identified isoforms originate from.

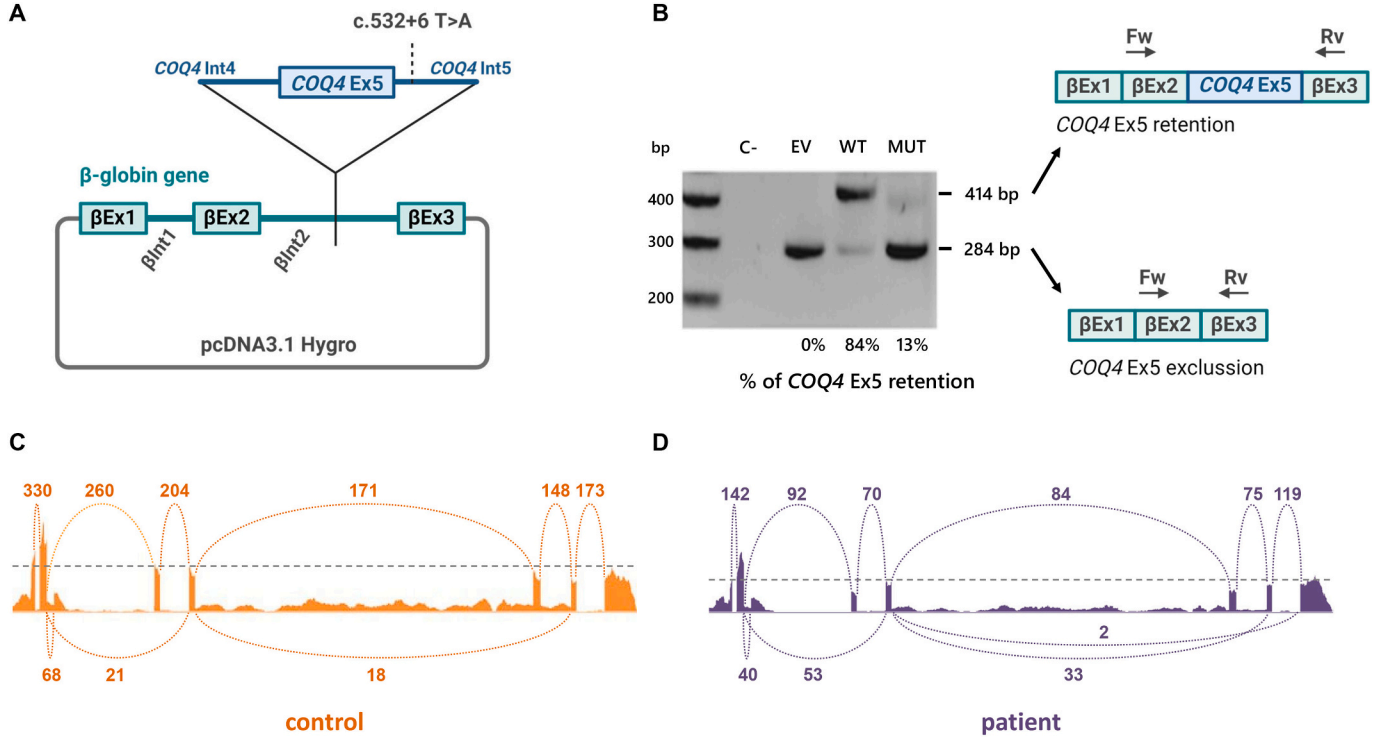

Fig. 3. RT-PCR analysis of the *COQ4* (c.532 + 6 T > A variant) minigene constructs expressed in HEK cells and RNAseq analysis of *COQ4* transcripts in PF and control fibroblasts. **A.** Schematic representation of the hybrid minigene constructs. The construct contains the closest exon to the variant, *COQ4* exon 5, and part of the upstream and downstream introns (± 100 bp). **B.** Cells were transfected with the mutant and the wild type constructs, and results of RT-PCR are shown in the agarose gel. The relative amounts of the different forms were determined by densitometry (percentages are shown on the bottom of the gel). A schematic representation of the spliced transcripts found is included. Ex, exon; C-, negative control of transfection; EV, transfection with empty β-globin-pCDNA3.1 vector; WT, wild-type construct; MUT, construct carrying c.532 + 6 T > A variant. **C.** RNAseq histogram plots of control RNA sample. The height of the histograms represents the read coverage. Splice junctions are displayed as arcs, each one with the number of reads observed for it. Canonical splicing events are indicated above the histograms, while alternative splicing events are displayed below them. **D.** RNAseq histogram plots of PF RNA sample. The height of the histograms represents the read coverage. Splice junctions are displayed as arcs, each one with the number of reads observed for it. Canonical splicing events are indicated above the histograms, while alternative splicing events are displayed below them.

Therefore, we used specific primers to amplify each *COQ4* whole processed transcript coming from either the c.23_33delTCCTCCGTCGG allele (forward deletion primer, del) or the c.532 + 6 T > A one (forward WT primer, WT) from the patient and control fibroblasts cDNA obtained from a total mRNA pool (Fig. 4A). Control samples amplified with the WT primer showed a predominant band corresponding to the *COQ4* whole transcript length. Amplification of control cDNA with the deletion primer resulted in a negligible band, probably unspecific. The proband sample amplified with the WT primer, which would only amplify the mRNA from the c.532 + 6 T > A allele, rendered 4 faint bands, suggesting that most of the transcripts coming from the intronic allele were aberrant. Surprisingly, the amplification of *COQ4* from the proband sample with the primer specific to the allele with the deletion in exon 1, rendered 3 clear bands, the longest corresponding to the whole-length transcript size. These three bands were common to the higher molecular weight bands amplified from the intronic variant (bands 1 to 3). Of note, some of these extra bands were also present in control samples amplified with the WT primer, although very faint.

Each resulting band was purified, subcloned, and sequenced to verify their identity (Fig. 5B). Band 1 contained the wild-type *COQ4* cDNA in the control cells amplified with the WT primer (isoform a) and the c.23_33delTCCTCCGTCGG cDNA allele in the proband's samples amplified with the deletion primer. Band 2, the most abundantly detected in PF amplified with deletion-specific primer, contained an isoform lacking exon 3 (isoform b). Band 3, lacking exons 3 and 5 (isoform d), was obtained in both the control (amplified with the WT primer) and the proband samples (amplified with both primers). Band 4, which was exclusively amplified from the intronic allele, contained an isoform lacking exons 3, 5, and 6 (isoform e). Isoforms b, d, and e are predicted to generate a frameshift (p.Asp68Glyfs*34) and lead to a truncated form of COQ4. Although not detected in the sequenced clones, a possible isoform lacking exon 5 would render a p.Gly135Argfs*5 frameshift allele (isoform c). This isoform could be present in band 2 as the predicted cDNA size is 668 bp and has been detected in a regular RT-PCR amplifying all the transcripts produced by the PF without distinguishing alleles (data not shown). To ascertain if the truncated proteins retained COQ4 function, isoforms a (full length), b (p.Asp68Glyfs*34), and c (p.Gly135Argfs*5) were cloned in pcDNA5 and transfected into HEK293T *COQ4 KO* Flp-In cells. As expected, only the whole transcript expression restored CoQ_{10} production (Fig. 4C) and suppressed the intermediary accumulation (Fig. 4D). These results suggest the prediction that the shorter isoforms enriched in the proband's cells are unable to replace the COQ4 function in CoQ_{10} biosynthesis when the full-length allele is absent.

3.7. Analysis of the predicted secondary COQ4 mRNA structure

Wild type and mutant genomic sequences containing 100 (Fig. S6A) or 200 nucleotides (Fig. S6B) upstream and downstream of the c.532 + 6 position were used as inputs for the RNAfold server [30] to predict the secondary structure of the pre-mRNA contributing to a state of minimum free energy. In both cases, the expected folding of the mutant sequence shows an evident divergence from the control sequence, changing the position and the pairing of some loops. Furthermore, the mutant sequence also reduces the pairing probabilities for several base pairs that are not only close to the change but also distant from it. When the whole mRNA molecule secondary structure is modeled, a milder effect of the intronic variant is observed, however (Fig. S7).

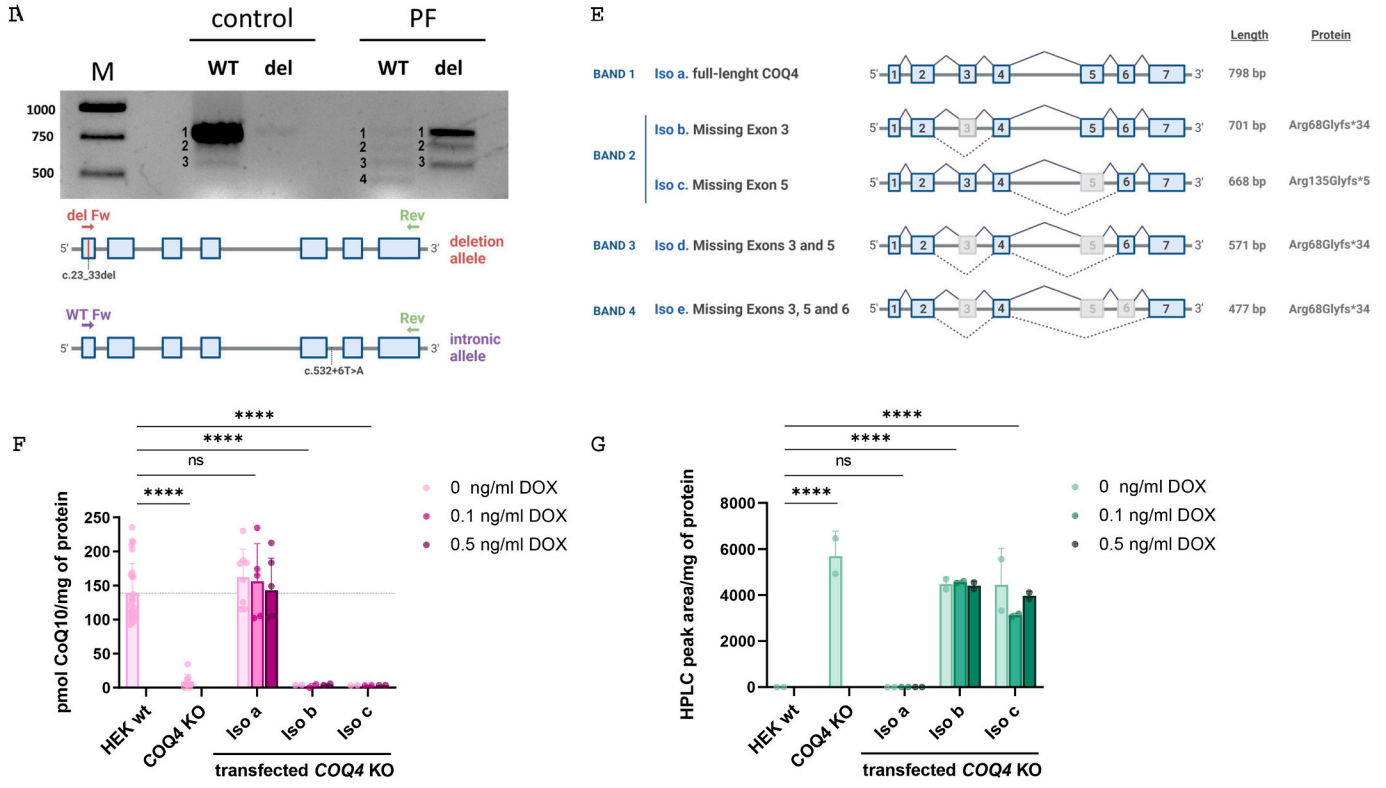

Fig. 4. Analysis of *COQ4* transcripts in PF and control fibroblasts. **A.** RT-PCR bands amplified with control (WT) and deletion (del) primers specific to the wild-type exon 1 from the c.532 + 6 T > A intronic allele and the c.23_33delTCCTCCGTCGG deletion allele, respectively (upper panel). Schematic representation of the PCR strategy (lower panel). **B.** Schematic representation of the spliced transcripts found in each band by sequencing of the amplified fragments. **C.** CoQ_{10} levels in HEK *COQ4* KO cells transfected with isoforms a to c (data expressed as mean ± SD; Two-way ANOVA, Dunnett's multiple comparison test (each transfected cell line *vs.* HEK WT); p values: ****, $p < 0.0001$). **D.** Intermediate in HEK *COQ4* KO cells transfected with isoforms a to c (data expressed as mean ± SD; Two-way ANOVA, Dunnett's multiple comparison test (each transfected cell line *vs.* HEK WT); p values: ****, $p < 0.0001$). Iso, isoform. PF, proband fibroblast. DOX, doxycycline; M, DNA 1Kb ladder.

4. Discussion

Here, we present a patient with compound heterozygous pathogenic variants in the *COQ4* gene, including c.532 + 6 T > A, a novel variant that could only be classified as disease-causing after several functional studies. The other variant, c.23_33delTCCTCCGTCGG, had already been described, and its mRNA was suggested to be subject to NMD and, thus, pathogenic [26].

Proband samples show reduced levels of COQ4 protein and decreased steady-state levels of CoQ_{10} and biosynthesis. Remarkably, the CoQ_{10} decrease in the proband's fibroblasts was associated with the accumulation of a compound with a different retention time from DMQ_{10}. DMQ_{10} is the substrate of COQ7 and has been previously identified in COQ7 and other COQ4 patients [31,32]. Instead, the subject accumulates a peak coincident with the form detected in *COQ4* KO cells and identified as 3-decaprenyl-4-hydroxybenzoate ($_{10}$P-HB), which is the substrate of COQ4, that has been recently demonstrated to be an oxidative decarboxylase in the CoQ biosynthesis pathway [14]. Small amounts of $_{10}$PPVA, an alternative substrate for COQ4 [10], are also detected in HEK293T KO *COQ4* cells, supporting that both pathways would operate in this cell model but possibly not in fibroblasts. COQ proteins have been shown to work in a complex, the Complex Q or CoQ synthome [33]. It has been suggested that dysregulation of one of the proteins could impact the stability of the assembly and the specific protein partners [34]. Thus, defects in COQ4 could induce a reduction in COQ7 levels in certain patients, which would explain the previously observed accumulation of DMQ_{10}. Variants that would disturb the complex assembly rather than COQ4 function would trigger the accumulation of intermediaries other than $_{10}$P-HB.

Biochemical analysis confirmed that CoQ_{10} deficiency in proband cells leads to suboptimal mitochondrial performance, explaining the pathophysiology of the disease. Altogether, our findings strongly suggest that the combination of c.532 + 6 T > A and c.23_33delTCCTCCGTCGG variants is disease-causing.

Pre-mRNA splicing is a central mechanism for producing functional proteins in eukaryotes. Nucleotide changes can modify this process, affecting the RNA processing in various ways, including exon skipping, intron retention or pseudoexon inclusion, and these diverse molecular phenotypes can lead to disease. It has been estimated that changes affecting pre-mRNA splicing are responsible for at least 15 % of disease-causing variants [2]. Most identified pathogenic variants causing Primary CoQ deficiency are located in the *COQ* genes coding sequence, but several variants have been described to affect mRNA processing. A homozygous splice-site variant and an exon skipping caused by a change in a predicted exon splice enhancer in the *COQ8A/ADCK3* gene were the first spliceogenic variants associated with CoQ deficiency [35]. Later, several other pathogenic variants were also identified in *COQ8A* and *COQ9* genes [36–38]. More recently, molecular characterization of 3 spliceogenic variants in *PDSS1* and *COQ5* genes in patients affected by retinitis pigmentosa have been reported [39]. However, CoQ_{10} levels were only measured in plasma, which is a poor indicator of the actual intracellular amounts, making the impact of the variants on CoQ_{10} biosynthesis unclear. The first *COQ4* spliceogenic variants have been recently reported in the literature [32,40]. The increasing identification of spliceogenic variants causing primary CoQ_{10} deficiency highlights the need for careful sequencing data generation and analysis to identify variants that could affect *COQ* genes' mRNA processing and render aberrant proteins. For this purpose, WGS should be more widely implemented.

The *COQ4* gene (ENSG00000167113) is composed of seven exons. Five different transcripts are listed in databases. However, only the one containing all exons (COQ4–201) is annotated as the primary transcript by Ensembl. The physiological significance of the other isoforms remains unclear. A dedicated RACE analysis performed by Casarin et al. revealed two isoforms, one of them lacking the nucleotides coding for the 24 initial amino acids, which is predicted to be part of the mitochondrial targeting sequence [41], but this isoform is absent from databases.

In silico analysis of the newly identified change c.532 + 6 T > A predicts moderate affection of the *COQ4* intron 5 donor site. Further molecular analysis was performed to confirm whether its pathogenicity relies on the alteration of pre-mRNA splicing and to determine the effect on *COQ4* mature mRNA specifically. The most used *in vitro* methods for validating splicing-defective mRNA are the expression and amplification of hybrid minigene constructs containing one or several exons flanked by part of the intronic sequences. Hybrid minigenes have been extensively used to functionally analyze the effects of genomic variations on splicing in single alleles [29,42,43]. A hybrid minigene construct containing *COQ4* exon 5 and the intronic flanking regions clearly showed the newly identified c.532 + 6 T > A variant impairs exon 5 splicing and is hypomorphic. Our results show that wild-type cells also generate some aberrant exon 5 skipping, suggesting that the c.532 + 6 T > A variant increases the frequency of a naturally occurring abnormal mRNA processing around intron 5. Although minigenes allow independent analysis of the effects on the splicing of single intronic/exonic changes, they can only partially analyze each variant separately from the natural whole mRNA context.

The advancement of high throughput transcriptomics, like RNA-Seq, along with the development of associated computational tools, have made it possible to quantitatively analyze splicing events in a genome-wide context with high resolution [44,45]. The quantification of RNA-seq reads of each *COQ4* exon and the frequency of the different splicing events surprisingly revealed a generally increased recurrence of incorrect splicing of the pre-mRNA transcript in the proband's cells. Intriguingly, although the putative spliceogenic variant c.532 + 6 T > A is located in the vicinity of the predicted donor site of intron 5, aberrant splicing events not only affect this intron but splicing combinations involving other exons/introns are clearly detected in PF. Of note, aberrant splicing of *COQ4* mRNA was also observed in control cells, although at a low frequency. Although the variant c.532 + 6 T > A is predicted to be spliceogenic by *in silico* tools and the minigene confirms a defect in the splicing of exon 5 in an *in vitro* context, we wanted to test whether some or all the other aberrant isoforms detected came from the alleles with the intronic change or the deletion.

As RNAseq reads are not long enough to distinguish between transcripts produced from each of the two alleles, we specifically amplified the transcript variants derived from each gene copy. Specific amplification of transcripts generated from each of the alleles showed that different aberrant isoforms are produced from both the c.532 + 6 T > A and, unexpectedly, the c.23_33delTCCTCCGTCGG allele, being 3 of these isoforms shared among them and also wild type cells. In all cases, isoforms derived from the intronic allele are less abundant than those from the deletion allele, suggesting the transcripts from this allele would be subjected to NMD. Although we cannot exclude the possibility of other isoforms, the variant c.532 + 6 T > A would specifically favor skipping of exons 3, 5, and 6 (isoform e). Thus, the intronic variant would impact the putative coordination of these exons'maturation. Again, in control cells, residual levels of aberrant splicing are also detected, which strongly supports that the *COQ4 missplicing* of the deletion allele is not due to an additional un-detected change in a different splice site of the gene. On the contrary, it would rather be the result of an exacerbation of a naturally occurring illegitimate mRNA maturation, possibly related to the long transcript length. However, we cannot exclude the possibility that the lower amplification of bands 2 and 3 in the control corresponds to a higher preference of primers for the more abundant full-length template (isoform a). Also, the predominant amplification of bands 2 and 3 from the deletion allele could be caused by higher availability of primers as the amplification of the full-length isoform is reduced compared to the control sample. Sondheimer et al. predicted that mRNA nonsense-mediated decay would be responsible for the deletion allele degradation. However, we cannot exclude the possibility that the primers designed for qPCR, which were not specified,

were specific to some of the skipped exons [26]. All the *misspliced* isoforms were predicted to render early truncated proteins, which were unable to restore CoQ_{10} biosynthesis in *COQ4* KO HEK293T cells.

Most mRNA sequences are predisposed to fold into large intramolecular secondary structures. This configuration has been suggested to have biological implications for various aspects of mRNA metabolism, including translation, splicing, and degradation, by influencing the binding and orientation of the proteins involved in these processes [46]. Alternative structures of mRNA that dictate the splicing outcome and, therefore, regulate the abundance of different isoforms have been investigated in various biological systems [47–49]. Although the minimum free energy prediction at 100 or 200 bp around the c.532 + 6 T > A intronic change foresees a modification in the mRNA structure, this variant does not have any apparent impact on the structure in the context of the whole pre-mRNA transcript, being thus unable to explain the specific splicing defect in PF. Instead, the 11-nt deletion in exon 1 has a slight impact on the whole pre-mRNA transcript structure, but it does not particularly influence the splicing compared with the control. Thus, the molecular process remains unexplained and needs further investigation. The reason why abnormal *COQ4* maturation occurs in control as well as in the deletion alleles and its physiological significance needs further analysis.

Most of the described *COQ4* patients have homozygous or compound heterozygous variants, with at least one allele harboring a missense, possibly hypomorphic, pathogenic variant. Our work suggests that the severity of the clinical symptoms and early fatal outcome in this patient could be associated with insufficient generation of wild-type transcripts from the intronic variant only and the absence of any hypomorphic copy produced from the deletion allele.

Elucidating the molecular mechanisms by which *COQ4* pre-mRNA is maturated and the consequences of the c.532 + 6 T > A and the c.23_33delTCCTCCGTCGG variants in this process could potentially pave the way for new therapies. Splice variants can be targeted with antisense oligonucleotides and are under active investigation for their application in personalized medicine [50], which potentially could be incorporated into the treatment options for primary CoQ deficiency caused by aberrant splicing of *COQ* genes in the future.

Funding

This work has been co-financed by the European Regional Development Fund (FEDER) and by the Department of Economic Transformation, Industry, Knowledge and Universities of the Government of Andalusia, within the framework of the operational program FEDER Andalusia 2014–2020. Thematic objective “01 - Strengthening research, technological development, and innovation” [Grant number P18-RT-4572] and the Specific objective 1.2.3. “Promotion and generation of frontier knowledge and knowledge oriented to the challenges of society, development of emerging technologies” [Grant number UPO-1265673]. FEDER co-financing percentage 80 %; EV had the support of Cariparo Foundation 20/19 FCR. This work was also supported by NIH awards R35GM131795 and funds from the BJC Investigator Program (to DJP). DJP is an investigator of the Howard Hughes Medical Institute.

CRediT authorship contribution statement

María Alcázar-Fabra: Writing – review & editing, Writing – original draft, Visualization, Methodology, Investigation, Formal analysis, Conceptualization. **Elsebet Østergaard:** Writing – review & editing, Writing – original draft, Methodology, Investigation, Formal analysis. **Daniel J.M. Fernández-Ayala:** Methodology, Investigation, Formal analysis, Data curation. **María Andrea Desbats:** Writing – review & editing, Methodology. **Valeria Morbidoni:** Methodology. **Laura Tomás-Gallado:** Methodology. **Laura García-Corzo:** Investigation. **María del Mar Blanquer-Roselló:** Investigation. **Abigail K. Bartlett:** Investigation. **Ana Sánchez-Cuesta:** Project administration, Investigation. **Lucía Sena:** Investigation. **Ana Cortés-Rodríguez:** Methodology, Investigation, Formal analysis. **María Victoria Cascajo-Almenara:** Investigation. **David J. Pagliarini:** Resources, Project administration, Investigation. **Eva Trevisson:** Writing – review & editing, Methodology, Investigation, Formal analysis, Conceptualization. **Sabine W. Gronborg:** Writing – review & editing, Writing – original draft, Supervision, Funding acquisition, Conceptualization. **Gloria Brea-Calvo:** Writing – review & editing, Writing – original draft, Visualization, Supervision, Project administration, Investigation, Funding acquisition, Formal analysis, Conceptualization.

Declaration of competing interest

The authors report no competing interests.

Data availability

Data will be made available on request.

Acknowledgments

We acknowledge the patient’s family, Prof Placido Navas, for the critical reading of the manuscript, Dr. Manuel Muñoz for discussions on the case, Dr. Pedro Patraquim for his assistance with RNA structure predictions and Dr. Rachel Guerra, who assisted with LC-MS measurements. The work at CABD benefits from the ‘Maria de Maetzu Units of Excellence Programm’ (CEX-2020-0011088-M) and the interdisciplinary framework provided by CSIC through the “LifeHUB.CSIC” initiative (PIE 202120E047-Conexiones-Life). Funding for open access publishing: Universidad Pablo de Olavide/CBUA.

Appendix A. Supplementary data

Supplementary data to this article can be found online at https://doi.org/10.1016/j.ymgmr.2024.101176.

References

[1] M.H. Wojcik, G. Lemire, E. Berger, M.S. Zaki, M. Wissmann, W. Win, S.M. White, B. Weisburd, D. Wieczorek, L.B. Waddell, J.M. Verboon, G.E. VanNoy, A. Töpf, T. Y. Tan, S. Syrbe, V. Strehlow, V. Straub, S.L. Stenton, H. Snow, M. Singer-Berk, J. Silver, S. Shril, E.G. Seaby, R. Schneider, V.G. Sankaran, A. Sanchis-Juan, K. A. Russell, K. Reinson, G. Ravenscroft, M. Radtke, D. Popp, T. Polster, K. Platzer, E. A. Pierce, E.M. Place, S. Pajusalu, L. Pais, K. Õunap, I. Osei-Owusu, H. Opperman, V. Okur, K.T. Oja, M. O’Leary, E. O’Heir, C.F. Morel, A. Merkenschlager, R. G. Marchant, B.E. Mangilog, J.A. Madden, D. MacArthur, A. Lovgren, J.P. Lerner-Ellis, J. Lin, N. Laing, F. Hildebrandt, J. Hentschel, E. Groopman, J. Goodrich, J. G. Gleeson, R. Ghaoui, C.A. Genetti, J. Gburek-Augustat, H.T. Gazda, V.S. Ganesh, M. Ganapathi, L. Gallacher, J.M. Fu, E. Evangelista, E. England, S. Donkervoort, S. DiTroia, S.T. Cooper, W.K. Chung, J. Christodoulou, K.R. Chao, L.D. Cato, K. M. Bujakowska, S.J. Bryen, H. Brand, C.G. Bönnemann, A.H. Beggs, S.M. Baxter, T. Bartolomaeus, P.B. Agrawal, M. Talkowski, C. Austin-Tse, R. Abou Jamra, H. L. Rehm, A. O’Donnell-Luria, Genome sequencing for diagnosing rare diseases, N. Engl. J. Med. 390 (2024) 1985–1997, https://doi.org/10.1056/NEJMoa2314761.

[2] N.G. Caminsky, E.J. Mucaki, P.K. Rogan, Interpretation of mRNA splicing mutations in genetic disease: review of the literature and guidelines for information-theoretical analysis, F1000Research 3 (2015), https://doi.org/10.12688/f1000research.5654.2.

[3] M. Aznaourova, N. Schmerer, B. Schmeck, L.N. Schulte, Disease-causing mutations and rearrangements in long non-coding RNA gene loci, Front. Genet. 11 (2020) 527484, https://doi.org/10.3389/fgene.2020.527484.

[4] A.C. Lionel, G. Costain, N. Monfared, S. Walker, M.S. Reuter, S.M. Hosseini, B. Thiruvahindrapuram, D. Merico, R. Jobling, T. Nalpathamkalam, G. Pellecchia, W.W.L. Sung, Z. Wang, P. Bikangaga, C. Boelman, M.T. Carter, D. Cordeiro, C. Cytrynbaum, S.D. Dell, P. Dhir, J.J. Dowling, E. Heon, S. Hewson, L. Hiraki, M. Inbar-Feigenberg, R. Klatt, J. Kronick, R.M. Laxer, C. Licht, H. MacDonald, S. Mercimek-Andrews, R. Mendoza-Londono, T. Piscione, R. Schneider, A. Schulze, E. Silverman, K. Siriwardena, O.C. Snead, N. Sondheimer, J. Sutherland, A. Vincent, J.D. Wasserman, R. Weksberg, C. Shuman, C. Carew, M.J. Szego, R. Z. Hayeems, R. Basran, D.J. Stavropoulos, P.N. Ray, S. Bowdin, M.S. Meyn, R. D. Cohn, S.W. Scherer, C.R. Marshall, Improved diagnostic yield compared with targeted gene sequencing panels suggests a role for whole-genome sequencing as a

first-tier genetic test, Genet. Med. 20 (2018) 435–443, https://doi.org/10.1038/gim.2017.119.
[5] M.J. Cormier, B.S. Pedersen, P. Bayrak-Toydemir, A.R. Quinlan, Combining genetic constraint with predictions of alternative splicing to prioritize deleterious splicing in rare disease studies, BMC Bioinformatics 23 (2022) 1–32, https://doi.org/10.1186/s12859-022-05041-x.
[6] L. Moyon, C. Berthelot, A. Louis, N.T.T. Nguyen, H.R. Crollius, Classification of non-coding variants with high pathogenic impact, PLoS Genet. 18 (2022) 1–20, https://doi.org/10.1371/journal.pgen.1010191.
[7] M. Alcázar-Fabra, F. Rodríguez-Sánchez, E. Trevisson, G. Brea-Calvo, Primary coenzyme Q deficiencies: a literature review and online platform of clinical features to uncover genotype-phenotype correlations, Free Radic. Biol. Med. 167 (2021) 141–180, https://doi.org/10.1016/j.freeradbiomed.2021.02.046.
[8] A.M. Awad, M.C. Bradley, L. Fernández-del-Río, A. Nag, H.S. Tsui, C.F. Clarke, Coenzyme Q $_{10}$ deficiencies: pathways in yeast and humans, Essays Biochem. 62 (2018) 361–376, https://doi.org/10.1042/EBC20170106.
[9] K. Bersuker, J.M. Hendricks, Z. Li, L. Magtanong, B. Ford, P.H. Tang, M.A. Roberts, B. Tong, T.J. Maimone, R. Zoncu, M.C. Bassik, D.K. Nomura, S.J. Dixon, J. A. Olzmann, The CoQ oxidoreductase FSP1 acts parallel to GPX4 to inhibit ferroptosis, Nature 575 (2019) 688–692, https://doi.org/10.1038/s41586-019-1705-2.
[10] M.J. Acosta Lopez, E. Trevisson, M. Canton, L. Vazquez-Fonseca, V. Morbidoni, E. Baschiera, C. Frasson, L. Pelosi, B. Rascalou, M.A. Desbats, M. Alcázar-Fabra, J. J. Ríos, A. Sánchez-García, G. Basso, P. Navas, F. Pierrel, G. Brea-Calvo, L. Salviati, Vanillic acid restores coenzyme Q biosynthesis and ATP production in human cells lacking COQ6, Oxidative Med. Cell. Longev. 2019 (2019) 1–11, https://doi.org/10.1155/2019/3904905.
[11] D. Herebian, L.C. López, F. Distelmaier, Bypassing human CoQ10 deficiency, Mol. Genet. Metab. 123 (2018) 289–291, https://doi.org/10.1016/j.ymgme.2017.12.008.
[12] J. Corral-Sarasa, J.M. Martínez-Gálvez, P. González-García, O. Wendling, L. Jiménez-Sánchez, S. López-Herrador, C.M. Quinzii, M.E. Díaz-Casado, L. C. López, 4-Hydroxybenzoic acid rescues multisystemic disease and perinatal lethality in a mouse model of mitochondrial disease, Cell Rep. (2024) 114148, https://doi.org/10.1016/j.celrep.2024.114148.
[13] D.J. Fernandez-Ayala, I. Guerra, S. Jimenez-Gancedo, M.V. Cascajo, A. Gavilan, S. Dimauro, M. Hirano, P. Briones, R. Artuch, R. De Cabo, L. Salviati, P. Navas, Survival transcriptome in the coenzyme Q10 deficiency syndrome is acquired by epigenetic modifications: a modelling study for human coenzyme Q10 deficiencies, BMJ Open 3 (2013), https://doi.org/10.1136/bmjopen-2012-002524.
[14] L. Pelosi, L. Morbiato, A. Burgardt, F. Tonello, A.K. Bartlett, R.M. Guerra, K. K. Ferizhendi, M.A. Desbats, B. Rascalou, M. Marchi, L. Vázquez-Fonseca, C. Agosto, G. Zanotti, M. Roger-Margueritat, M. Alcázar-Fabra, L. García-Corzo, A. Sánchez-Cuesta, P. Navas, G. Brea-Calvo, E. Trevisson, V.F. Wendisch, D. J. Pagliarini, L. Salviati, F. Pierrel, COQ4 is Required for the Oxidative Decarboxylation of the C1 Carbon of Coenzyme Q in Eukaryotic Cells, 2023, https://doi.org/10.1101/2023.11.13.566839, 2023.11.13.566839.
[15] A. Berardo, C.M. Quinzii, Redefining infantile-onset multisystem phenotypes of coenzyme Q10-deficiency in the next-generation sequencing era, J. Transl. Genet. Genom. (2020), https://doi.org/10.20517/jtgg.2020.02.
[16] F.A. Ran, P.D. Hsu, J. Wright, V. Agarwala, D.A. Scott, F. Zhang, Genome engineering using the CRISPR-Cas9 system, Nat. Protoc. 8 (2013) 2281–2308, https://doi.org/10.1038/nprot.2013.143.
[17] J.C. Rodríguez-Aguilera, A.B. Cortés, D.J.M. Fernández-Ayala, P. Navas, Biochemical assessment of coenzyme Q10 deficiency, J. Clin. Med. 6 (2017) 27, https://doi.org/10.3390/jcm6030027.
[18] D.J. Fernandez-Ayala, G. Brea-Calvo, G. Lopez-Lluch, P. Navas, Coenzyme Q distribution in HL-60 human cells depends on the endomembrane system, Biochim. Biophys. Acta 1713 (2005) 129–137, https://doi.org/10.1016/j.bbamem.2005.05.010.
[19] R. Leman, P. Gaildrat, G.L. Gac, C. Ka, Y. Fichou, M.P. Audrezet, V. Caux-Moncoutier, S.M. Caputo, N. Boutry-Kryza, M. Léone, S. Mazoyer, F. Bonnet-Dorion, N. Sevenet, M. Guillaud-Bataille, E. Rouleau, B.B. De Paillerets, B. Wappenschmidt, M. Rossing, D. Muller, V. Bourdon, F. Revillon, M.T. Parsons, A. Rousselin, G. Davy, G. Castelain, L. Castéra, J. Sokolowska, F. Coulet, C. Delnatte, C. Férec, A.B. Spurdle, A. Martins, S. Krieger, C. Houdayer, Novel diagnostic tool for prediction of variant spliceogenicity derived from a set of 395 combined in silico/in vitro studies: an international collaborative effort, Nucleic Acids Res. 46 (2018) 7913–7923, https://doi.org/10.1093/nar/gky372.
[20] K. Jaganathan, S. Kyriazopoulou Panagiotopoulou, J.F. McRae, S.F. Darbandi, D. Knowles, Y.I. Li, J.A. Kosmicki, J. Arbelaez, W. Cui, G.B. Schwartz, E.D. Chow, E. Kanterakis, H. Gao, A. Kia, S. Batzoglou, S.J. Sanders, K.K.-H., Farh, predicting splicing from primary sequence with deep learning, Cell 176 (2019) 535–548.e24, https://doi.org/10.1016/j.cell.2018.12.015.
[21] F.-O. Desmet, D. Hamroun, M. Lalande, G. Collod-Béroud, M. Claustres, C. Béroud, Human splicing finder: an online bioinformatics tool to predict splicing signals, Nucleic Acids Res. 37 (2009) e67, https://doi.org/10.1093/nar/gkp215.
[22] N. Scalzitti, A. Kress, R. Orhand, T. Weber, L. Moulinier, A. Jeannin-Girardon, P. Collet, O. Poch, J.D. Thompson, Spliceator: multi-species splice site prediction using convolutional neural networks, BMC Bioinformatics 22 (2021) 561, https://doi.org/10.1186/s12859-021-04471-3.
[23] S. Brunak, J. Engelbrecht, S. Knudsen, Prediction of human mRNA donor and acceptor sites from the DNA sequence, J. Mol. Biol. 220 (1991) 49–65, https://doi.org/10.1016/0022-2836(91)90380-o.
[24] M. Cassina, C. Cerqua, S. Rossi, L. Salviati, A. Martini, M. Clementi, E. Trevisson, A synonymous splicing mutation in the SF3B4 gene segregates in a family with highly variable Nager syndrome, Eur. J. Hum. Genet. 25 (2017) 371–375, https://doi.org/10.1038/ejhg.2016.176.
[25] H. Thorvaldsdóttir, J.T. Robinson, J.P. Mesirov, Integrative genomics viewer (IGV): high-performance genomics data visualization and exploration, Brief. Bioinform. 14 (2013) 178–192, https://doi.org/10.1093/bib/bbs017.
[26] N. Sondheimer, S. Hewson, J.M. Cameron, G.R. Somers, J.D. Broadbent, M. Ziosi, C.M. Quinzii, A.B. Naini, Novel recessive mutations in COQ4 cause severe infantile cardiomyopathy and encephalopathy associated with CoQ 10 deficiency, Mol. Genet. Metab. Rep. 12 (2017) 23–27, https://doi.org/10.1016/j.ymgmr.2017.05.001.
[27] G. Brea-Calvo, T.B. Haack, D. Karall, A. Ohtake, F. Invernizzi, R. Carrozzo, L. Kremer, S. Dusi, C. Fauth, S. Scholl-Bürgi, E. Graf, U. Ahting, N. Resta, N. Laforgia, D. Verrigni, Y. Okazaki, M. Kohda, D. Martinelli, P. Freisinger, T. M. Strom, T. Meitinger, C. Lamperti, A. Lacson, P. Navas, J.A. Mayr, E. Bertini, K. Murayama, M. Zeviani, H. Prokisch, D. Ghezzi, COQ4 mutations cause a broad spectrum of mitochondrial disorders associated with CoQ10 deficiency, Am. J. Hum. Genet. 96 (2015) 309–317, https://doi.org/10.1016/j.ajhg.2014.12.023.
[28] D. Herebian, A. Seibt, S.H.J. Smits, G. Bünning, C. Freyer, H. Prokisch, D. Karall, A. Wredenberg, A. Wedell, L.C. López, E. Mayatepek, F. Distelmaier, Detection of 6-demethoxyubiquinone in CoQ10 deficiency disorders: insights into enzyme interactions and identification of potential therapeutics, Mol. Genet. Metab. 121 (2017) 216–223, https://doi.org/10.1016/j.ymgme.2017.05.012.
[29] V. Morbidoni, E. Baschiera, M. Forzan, V. Fumini, D.S. Ali, G. Giorgi, L. Buson, M. A. Desbats, M. Cassina, M. Clementi, L. Salviati, E. Trevisson, Hybrid minigene assay: an efficient tool to characterize mrna splicing profiles of nf1 variants, Cancers 13 (2021) 1–26, https://doi.org/10.3390/cancers13050999.
[30] R. Lorenz, S.H. Bernhart, C. Höner Zu Siederdissen, H. Tafer, C. Flamm, P. F. Stadler, I.L. Hofacker, ViennaRNA Package 2.0, Algorit. Mol. Biol. 6 (2011) 26, https://doi.org/10.1186/1748-7188-6-26.
[31] L. Laugwitz, A. Seibt, D. Herebian, S. Peralta, I. Kienzle, R. Buchert, R. Falb, D. Gauck, A. Müller, M. Grimmel, S. Beck-Woedel, J. Kern, K. Daliri, P. Katibeh, K. Danhauser, S. Leiz, V. Alesi, F. Baertling, G. Vasco, R. Steinfeld, M. Wagner, A. O. Caglayan, H. Gumus, M. Burmeister, E. Mayatepek, D. Martinelli, P. M. Tamhankar, V. Tamhankar, P. Joset, K. Steindl, A. Rauch, P.E. Bonnen, T. Froukh, S. Groeschel, I. Krägeloh-Mann, T.B. Haack, F. Distelmaier, Human COQ4 deficiency: delineating the clinical, metabolic and neuroimaging phenotypes, J. Med. Genet. (2021), https://doi.org/10.1136/jmedgenet-2021-107729 jmedgenet-2021-107729.
[32] I. Cordts, L. Semmler, J. Prasuhn, A. Seibt, D. Herebian, T. Navaratnarajah, J. Park, N. Deininger, L. Laugwitz, S.L. Göricke, P. Lingor, N. Brüggemann, A. Münchau, M. Synofzik, D. Timmann, J.A. Mayr, T.B. Haack, F. Distelmaier, M. Deschauer, Bi-allelic COQ4 variants cause adult-onset Ataxia-spasticity Spectrum disease, Mov. Disord. 37 (2022) 2147–2153, https://doi.org/10.1002/mds.29167.
[33] R.M. Guerra, D.J. Pagliarini, Coenzyme Q biochemistry and biosynthesis, Trends Biochem. Sci. 48 (2023) 463–476, https://doi.org/10.1016/j.tibs.2022.12.006.
[34] J.A. Stefely, D.J. Pagliarini, Biochemistry of mitochondrial coenzyme Q biosynthesis, Trends Biochem. Sci. 0 (2017) 1–20, https://doi.org/10.1016/j.tibs.2017.06.008.
[35] C. Lagier-Tourenne, M. Tazir, L.C. Lopez, C.M. Quinzii, M. Assoum, N. Drouot, C. Busso, S. Makri, L. Ali-Pacha, T. Benhassine, M. Anheim, D.R. Lynch, C. Thibault, F. Plewniak, L. Bianchetti, C. Tranchant, O. Poch, S. DiMauro, J. L. Mandel, M.H. Barros, M. Hirano, M. Koenig, ADCK3, an ancestral kinase, is mutated in a form of recessive Ataxia associated with coenzyme Q10 deficiency, Am. J. Hum. Genet. 82 (2008) 661–672, https://doi.org/10.1016/j.ajhg.2007.12.024.
[36] J.C. Jacobsen, W. Whitford, B. Swan, J. Taylor, D.R. Love, R. Hill, S. Molyneux, P. M. George, R. Mackay, S.P. Robertson, R.G. Snell, K. Lehnert, Compound Heterozygous Inheritance of Mutations in Coenzyme Q8A Results in Autosomal Recessive Cerebellar Ataxia and Coenzyme Q10 Deficiency in a Female Sib-Pair, in: JIMD Reports, Springer, Berlin, Heidelberg, 2017, pp. 31–36, https://doi.org/10.1007/8904_2017_73.
[37] J.K. Cullen, N.A. Murad, A. Yeo, M. McKenzie, M. Ward, K.L. Chong, N.L. Schieber, R.G. Parton, Y.C. Lim, E. Wolvetang, G.J. Maghzal, R. Stocker, M.F. Lavin, AarF domain containing kinase 3 (ADCK3) mutant cells display signs of oxidative stress, defects in mitochondrial homeostasis and lysosomal accumulation, PLoS One 11 (2016) 1–28, https://doi.org/10.1371/journal.pone.0148213.
[38] A.C. Smith, Y. Ito, A. Ahmed, J.A. Schwartzentruber, C.L. Beaulieu, E. Aberg, J. Majewski, D.E. Bulman, K. Horsting-wethly, D.V. Koning, C.C. Consortium, R. J. Rodenburg, K.M. Boycott, L.S. Penney, A family segregating lethal neonatal coenzyme Q 10 deficiency caused by mutations in COQ9, J. Inherit. Metab. Dis. 41 (4) (2018) 719–729, https://doi.org/10.1007/s10545-017-0122-7.
[39] N. Jurkute, F. Cancellieri, L. Pohl, C.H.Z. Li, R.A. Heaton, J. Reurink, J. Bellingham, M. Quinodoz, G. Yioti, M. Stefaniotou, M. Weener, T. Zuleger, T. B. Haack, K. Stingl, J.C. Ambrose, P. Arumugam, R. Bevers, M. Bleda, F. Boardman-Pretty, C.R. Boustred, H. Brittain, M.A. Brown, M.J. Caulfield, G.C. Chan, A. Giess, J.N. Griffin, A. Hamblin, S. Henderson, T.J.P. Hubbard, R. Jackson, L.J. Jones, D. Kasperaviciute, M. Kayikci, A. Kousathanas, L. Lahnstein, A. Lakey, S.E.A. Leigh, I.U.S. Leong, F.J. Lopez, F. Maleady-Crowe, M. McEntagart, F. Minneci, J. Mitchell, L. Moutsianas, M. Mueller, N. Murugaesu, A.C. Need, P. O'Donovan, C.A. Odhams, C. Patch, D. Perez-Gil, M.B. Pereira, J. Pullinger, T. Rahim, A. Rendon, T. Rogers, K. Savage, K. Sawant, R.H. Scott, A. Siddiq, A. Sieghart, S.C. Smith, A. Sosinsky, A. Stuckey, M. Tanguy, A.L. Taylor Tavares, E.R.A. Thomas, S.R. Thompson, A. Tucci, M.J. Welland, E. Williams, K. Witkowska, S.M. Wood, M. Zarowiecki, C. B. Hoyng, O.A. Mahroo, I. Hargreaves, F.L. Raymond, M. Michaelides, C. Rivolta, S. Kohl, S. Roosing, A.R. Webster, G. Arno, Biallelic variants in coenzyme Q10

biosynthesis pathway genes cause a retinitis pigmentosa phenotype, Npj, Genom. Med. 7 (2022), https://doi.org/10.1038/s41525-022-00330-z.
[40] X. Lin, J. Jiang, D. Hong, K. Lin, J. Li, Y. Chen, Y. Qiu, Z. Wang, Y. Liao, K. Yang, Y. Shi, M. Wang, S. Hsu, S. Hong, Y. Zeng, X. Chen, N. Wang, Y. Lee, W. Chen, Biallelic COQ4 variants in hereditary spastic paraplegia: clinical and molecular characterization, Mov. Disord. 39 (2024) 152–163, https://doi.org/10.1002/mds.29664.
[41] A. Casarin, J.C. Jimenez-Ortega, E. Trevisson, V. Pertegato, M. Doimo, M. L. Ferrero-Gomez, S. Abbadi, R. Artuch, C. Quinzii, M. Hirano, G. Basso, C. S. Ocaña, P. Navas, L. Salviati, Functional characterization of human COQ4, a gene required for coenzyme Q10 biosynthesis, Biochem. Biophys. Res. Commun. 372 (2008) 35–39, https://doi.org/10.1016/j.bbrc.2008.04.172.
[42] E. Fraile-Bethencourt, B. Díez-Gómez, V. Velásquez-Zapata, A. Acedo, D.J. Sanz, E. A. Velasco, Functional classification of DNA variants by hybrid minigenes: identification of 30 spliceogenic variants of BRCA2 exons 17 and 18, PLoS Genet. 13 (2017) e1006691, https://doi.org/10.1371/journal.pgen.1006691.
[43] E. Fraile-Bethencourt, A. Valenzuela-Palomo, B. Díez-Gómez, M.J. Caloca, S. Gómez-Barrero, E.A. Velasco, Minigene splicing assays identify 12 Spliceogenic variants of BRCA2 exons 14 and 15, Front. Genet. 10 (2019) 503, https://doi.org/10.3389/fgene.2019.00503.
[44] S. Zhao, Alternative splicing, RNA-seq and drug discovery, Drug Discov. Today 24 (2019) 1258–1267, https://doi.org/10.1016/j.drudis.2019.03.030.
[45] A. Mehmood, A. Laiho, M.S. Venäläinen, A.J. McGlinchey, N. Wang, L.L. Elo, Systematic evaluation of differential splicing tools for RNA-seq studies, Brief. Bioinform. 21 (2020) 2052–2065, https://doi.org/10.1093/bib/bbz126.
[46] W.J.C. Lai, M. Kayedkhordeh, E.V. Cornell, E. Farah, S. Bellaousov, R. Rietmeijer, E. Salsi, D.H. Mathews, D.N. Ermolenko, mRNAs and lncRNAs intrinsically form secondary structures with short end-to-end distances, Nat. Commun. 9 (2018), https://doi.org/10.1038/s41467-018-06792-z.
[47] M.B. Warf, J.A. Berglund, Role of RNA structure in regulating pre-mRNA splicing, Trends Biochem. Sci. 35 (2010) 169–178, https://doi.org/10.1016/j.tibs.2009.10.004.
[48] P.J. Tomezsko, V.D.A. Corbin, P. Gupta, H. Swaminathan, M. Glasgow, S. Persad, M.D. Edwards, L. Mcintosh, A.T. Papenfuss, A. Emery, R. Swanstrom, T. Zang, T.C. T. Lan, P. Bieniasz, D.R. Kuritzkes, A. Tsibris, S. Rouskin, Determination of RNA structural diversity and its role in HIV-1 RNA splicing, Nature 582 (2020) 438–442, https://doi.org/10.1038/s41586-020-2253-5.
[49] P.J. Shepard, K.J. Hertel, Conserved RNA secondary structures promote alternative splicing, RNA 14 (2008) 1463–1469, https://doi.org/10.1261/rna.1069408.
[50] A. Martinez-Pizarro, L.R. Desviat, RNA solutions to treat inborn errors of metabolism, Mol. Genet. Metab. 136 (2022) 289–295, https://doi.org/10.1016/j.ymgme.2022.07.006.
[52] Azizia Wahedi, Sniya Sudhakar, Amanda Lam, Jose Ignacio Rodriguez Ciancio, Philippa Mills, Paul Gissen, Alice Gardham, Jogesh Kapadia, Jane Hassell, Simon Heales, Shamima Rahman, Clinical Features, Biochemistry, Imaging, and Treatment Response in a Single-Center Cohort With Coenzyme Q10 Biosynthesis Disorders, Neurol Genet 10 (6) (2024) e200209, https://doi.org/10.1212/NXG.0000000000200209.